AADE-24-FTCE-006

Self-adaptive Behavior of Shape Memory Particles During Lost Circulation Prevention

Weibin Zha, Songbing Yan, Meng Lu, Janine Shipman, Fucheng Liu, CNPC USA; Xianbin Zhang, Bohai Drilling Technology

Abstract

In this research, we developed heat-stimulated thermoplastic and thermoset shape memory polymers (SMPs) with very good shape recovery rate. Thermoplastic SMP was preprogrammed by extension while the thermoset one was preprogrammed by compression. Both preprogrammed and un-preprogrammed strips/plates made with these two materials were cut into high-aspect ratio particles. Two separate aliquots of a generic water-based mud were mixed with these particles, respectively, to test lost circulation prevention capability of these particles. Two new lost circulation test fixtures were designed and set-up to show the self-adaptive effect of shape changing during lost circulation prevention.

Thermoplastic shape memory has a glass transition temperature (T_g) of 70-90 ºC and its particles can seal a standard slotted lost circulation disk up to 140 ºC under 10 MPa. The T_g of thermoset polymer is around 100-120 ºC and it can seal the disk up to 180 ºC under 10 MPa. In our specially designed test fixture, which is a tapered 7.25 inch-long slot, un-programmed particles performed just like other usual polymer particles without shape changing before the testing temperature reached transition temperature, As temperature increased to transition region, preprogrammed high-aspect-ratio (HAR) particles changed to low-aspect ratio (LAR) and moved into the deeper and narrower side of the slot and built-up pressure again. This self-adaptive property is unique and important in lost circulation prevention.

This is the first observation of self-adaptive behavior of SMP particles in lost circulation test. This self-adaptive behavior makes these particles seal a much broader range of fractures so that it makes it easier to do particle size optimization.

Introduction

Lost circulation in drilling operations occurs when drilling fluids, or mud, intended to circulate in the wellbore to cool and clean the drill bit escape into the formation. Lost circulation incidents tend to happen more often when drilling challenging wells, such as extended reach wells or deep-water wells, as the operational mud weight window narrows. The mud weight window is the range of mud weights that can be used without causing lost circulation or wellbore instability. The procedure to correct lost circulation typically involves implementing various techniques and materials to regain control over the wellbore and prevent further mud loss. This procedure is considered one of the major contributors to drilling non-productive time (NPT) and is always associated with huge financial cost.

The most commonly used method to correct lost circulation is to use Lost Circulation Materials (LCMs) (Al-Arfaj et. al., 2018). LCMs are additives mixed with the drilling mud to plug or bridge the fractures or pores in the formation, thereby stopping or reducing mud loss.

Due to the different properties of LCMs and how these properties contribute to their various applications, Alsaba etc. classified LCMs into 7 categories (Alsaba et. al., 2014): granular, flaky, fibrous, LCM- mixture, acid soluble, high fluid loss LCM's squeezes (HFLS), swellable/hydratable LCM's, and nanoparticles. Since the physical appearance and the size of SMP particles that we will discuss in this paper are granular, flaky, fibrous, and their mixture, we will look into more details about these categories.

To categorize a particle into granular, flaky or fibrous depends on the aspect ratio of the particle. The aspect ratio of a shape is the ratio of its longer dimension to its shorter dimension. For granular particles, the aspect ratio will be close to one, even though they are not necessarily in perfect spherical shape. Flaky and fibrous type particles have much higher aspect ratio.

Granular materials include graphite, nut shells, sized calcium carbonate, gilsonite, course bentonite etc. Due to their rigidity, this type of material has higher crushing resistance. They are often used for wellbore strengthening applications.

Flaky materials are thin and flat in shape, with a large surface area[3]. Flaky materials include cellophane, mica, cottonseed hulls, vermiculite, corn cobs, and flaked calcium carbonate.

Fibrous materials include cellulose fibers, nylon fibers, mineral fibers, saw dust, and shredded paper. Fibrous particles are long, slender, and flexible in various sizes and lengths (Schlumberger, 2014). This type of material may have a little degree of stiffness and will form a "mat-like" bridge when used to reduce the losses into fractures or vugular formations (Howard et. al., 1951). The ability to form a "mat-like" bridge serves as a skeleton for smaller particles in the drilling fluids to deposit and form a seal (Nayberg et. al., 1986).

In most cases, a mixture of different types of LCMs was observed with better performance in mitigating losses due to the different properties and particle sizes of the mixed LCMs (Withfill et. al., 2008; Van Oort et. al., 2009). These blends contain optimized types and particle size distribution (PSD) that have been evaluated in various lab tests to prove their ability in sealing wide range of fracture sizes.

PSD of LCM is the most important criterion on which treatments are designed. Different researchers have published different model predictions and different experimental results. Tran et. al. 2009 carried out experimental studies correlating plugging time and particle size to pore throat size as a function of particle volume fraction Reynolds number. They concluded that the very commonly used 1/3 plugging rule is valid for limited conditions and is not adequate for general applications.

$$D(50) = \frac{\gamma}{3} = \frac{Fracture\ opening\ size}{3}$$

Lee et. al. 2020 found that effective fracture sealing is achieved with bimodally distributed LCMs, where effectiveness is related to the packing efficiency of specifically sized particles. Results from Omid Razavi et. al., 2016 also suggest that bimodal PSD has a clear strengthening advantage over a unimodal PSD.

LCM performance evaluation tests

Laboratory evaluation of LCMs is a crucial step to investigate their feasibility and durability prior to field applications. The most frequently used testing method is to use Permeability Plugging Tester (PPT) as shown in Figure 1 (a) which is a modification of the HTHP fluid loss cell. The drilling fluid with LCMs is pumped from the bottom with pre-determined pressure difference to be pushed upward against a slotted disk as shown in Figure 1(b) that can simulate the natural and induced fractures. The testing is deemed successful if the LCM is able to plug the disc and stop the mud losses entirely or the fluid loss is less than a targeted volume after 30 minutes. This method could be suitable to evaluate the performance of SMP LCM since temperature and pressure can be accurately controlled.

Loeppke et. al., 1990; Withfill et. al. 2003 developed larger scale setups that can simulate field conditions better. These customized testers use a reservoir to store mud containing LCM and pump the mud through a circulating loop. The fluid passes specially designed openings to simulate fractures. This type of test simulates the actual field environment as the fluid has the opportunity to escape into fractures after being circulated in the mud system. We also used a derivative of this design for our test method. bb

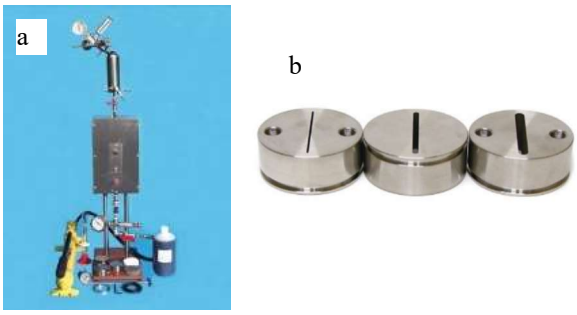

Figure 1 a) Particle Plugging Test Apparatus (OFITE®); b) slotted disk.

Shape memory polymer

Shape memory polymers (SMPs) are a class of smart materials that can "remember" a specific shape and return to it when triggered by an external stimulus. These polymers exhibit a unique property known as the shape memory effect (SME), which allows them to undergo a reversible change in shape in response to external stimuli such as heat, light, or pH.

The most common type of SMPs relies on temperature as the triggering stimulus. There are two main phases in the shape memory process shown in Figure 2 (Prathumrat et. al., 2022) above.

Programming Phase: During this phase, the polymer is deformed into a temporary shape at an elevated temperature which is above the transition temperature (T_{trans}). In most cases, T_{trans} is the same as the glass transition temperature (T_g) of the polymer matrix. The polymer is then cooled down below T_{trans} while maintaining the temporary shape. This process fixes the temporary shape in the polymer's memory. During this procedure, some energy is stored in the form of reversible polymer chain deformation. But not all the polymer chain deformations are reversible. Only part of the deformations is reversible.

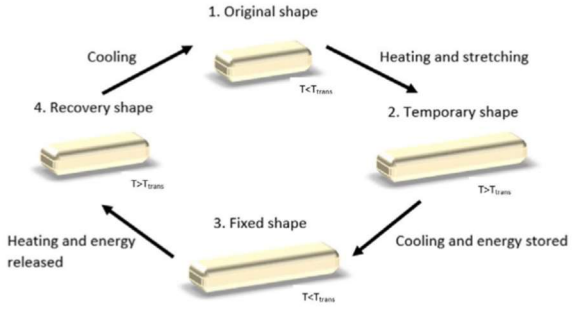

Figure 2 Schematic representation of the deformation of a shape memory cycle adapted from reference 13.

Recovery Phase: When the pre-programmed polymer is exposed to the triggering stimulus (usually heating, $T \geq T_{trans}$), part of the deformation returns to its original, permanent shape and the stored energy releases.

The ratio between reversible and total deformation is a very important indicator of the performance of SMPs. We usually measure the dimensions of the sample in its original state, after programming and after recovery to determine the recovery rate. The recovery rate can be calculated with the equation below:

$$Recovery\ Rate = \frac{Lr - Lp}{Lo - Lp}$$

Lo is the original dimension that could be the length or thickness of the sample. Lp is the dimension after programming. Lr is the dimension after recovery phase.

When a SMP undergoes the recovery phase, the force exerted during the process is often referred to as the recovery force. The recovery force of SMPs is another crucial characteristic that defines their ability to return to their original shape during the recovery phase of the shape memory effect. Just like recovery rate, the recovery force is influenced by various factors, including the polymer's chemical composition, molecular structure, processing conditions, and the specific triggering stimulus.

SMPs with temperature as an external stimulus can be either thermoset or thermoplastic. Thermoset SMPs usually have higher stiffness, strength, thermostability and dimensional stability due to the existence of chemically crosslinking bonds as compared to thermoplastic SMPs. During the programming phase, the crystal structure or the hard block of thermoplastic SMPs could be affected so that the shape recovery rate is usually lower than that of thermoset SMPs. So thermoset SMPs are preferred in engineering structures. Thermoplastic SMPs are relatively easier to process and can tolerate large deformation during the programming phase.

SMPs find applications in various fields, including biomedical devices (He et. al., 2019; Xiao et. al., 2019; Worch et. al.,2020), aerospace engineering (Liu et. al., 2014; Arun et. al., 2019; Dao et. al., 2018), textiles, robotics, and other high tech or high value-added industries where the ability to switch between different shapes can be advantageous. Their unique properties make them valuable in situations where precise control over shape-changing materials is required. Recently, SMPs have attracted attention from the petroleum/sub-surface drilling realm, especially in the areas focusing on LCM application and wellbore strengthening. Magzoub and Li et al. [20] investigated using expandable SMPs in geothermal drilling. They found that SMPs have great potential for sealing large fractures by using formation temperature to trigger the thermoset polymer at a preprogrammed point. The recovered shape and size worked as a bridging material. They developed a dynamic LCM testing unit to evaluate the LCM performance of SMPs.

Santos, Li et. al., 2016, 2018, 2020, 2021 published a series of research papers and presentations about using expandable SMPs to develop expandable proppant and expandable cement materials. They claimed that the proppant could expand in size when placed inside the fracture to enhance fracture overall permeability and consequently improve production of hydraulically fractured wells. The expansion, triggered by high temperature, resulted in up to 100% increase in permeability. This new SMP additive can also enhance the mechanical properties of the class G cement in terms of compressive strength, flexure strength, ductility and resiliency.

Wang et. al., 2016 used SMPs to provide downhole sand control in an open hole environment. When expanded as designed, the SMP conformed to the sand face, providing a positive stress on the immediate wellbore area, stabilizing the wellbore and preventing sand movement. Its sand retention and filtration capabilities are equivalent or superior to those of open hole gravel packing.

Shojaei et. al., 2020 also published a patent about using SMPs in wellbore servicing fluids without laboratory data.

In this research, we developed heat-stimulated thermoplastic and thermoset SMPs with very good shape recovery rate. We found an efficient way to program both materials in a bulk volume and then cut them into particles with HAR. This project was focused on lost circulation evaluation tests with programmed and un-programmed particles to see the difference. We also developed two new lost circulation tests to show the self-adaptive effect of shape changing during lost circulation prevention.

Experimental results

Materials and programming

We developed two SMPs, Thermoset A and Thermoplastic B. The physical properties of these two materials are list in Table 1 below:

Table 1 Physical properties of shape memory materials.

Properties	**Thermoset A**	**hermoplastic B**
Hardness Shore D 20 ℃）	85	78
Tensile Strength（MPa）	55	68.5
Elongation at Break （%）	20	400
Density	1.2	1.2
Glass Transition Temperature (℃)	90-130	70-90

Due to the significant differences in the physical properties of thermoset A and thermoplastic B, we have developed distinct programming processes for these two materials. The elongation at break of thermoset A is only around 20%, making it impractical to induce large deformations using a stretching method, resulting in limited shape memory recovery. Therefore, we employed a compression method, where the sample is compressed along its thickness direction under heating.

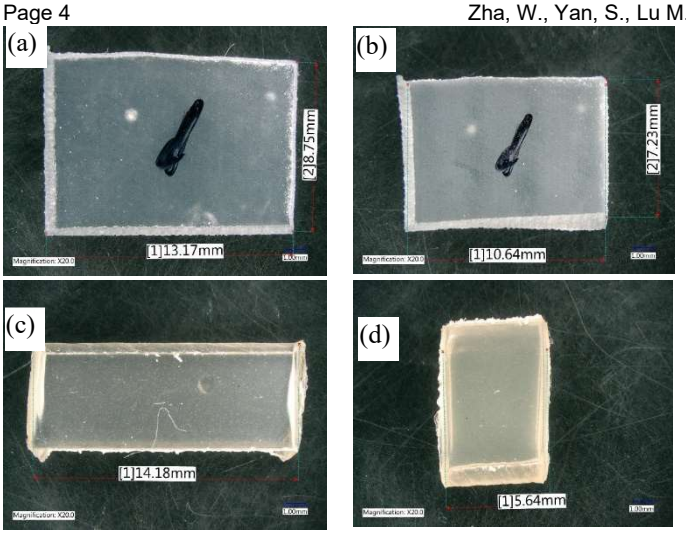

Figure 3 a) programmed A; b) recovered A; c) programmed B; d) recovered B.

For thermoplastic B, since the elongation at break is larger than 400%, we employed a stretching method.

To program thermoset A material, we used an Instron mechanical testing instrument with a heated oven in the lab by replacing the tension kit with a compression kit.

To program thermoplastic B, we made strips first with the injection molding method. Then the strips were stretched to 300% of their original length in the oven at 110°C followed by quick quenching. Figure 3 shows the dimensions of the programmed pieces before and after recovery. Even though the thermoplastic B sample seems to have recovered much more than thermoset A sample, thermoset B sample has a higher calculated recovery rate. This happened due to the larger initial deformation of thermoplastic sample during the programming phase. Both materials have a recovery rate higher than 85%.

Pelletizing

Ideally, we could pelletize the material first then do the programming one particle at a time. But programming each particle is impractical and the particles made that way will not be randomly shaped which is critical for good sealing capability. So, we chose to program a relatively big piece then pelletize it with a cutting mill to make the particles for our tests.

After programming, we put programmed big pieces into a Retsch SM 100 cutting mill to pelletize both materials. Because thermoset A has a higher T_g, it is relatively brittle at room temperature, so a lot of small particles or powder were created using this method. We used sieves to separate them into different size groups. Figure 4a shows two groups of separated particles. The smaller ones are less than 0.6 mm while the bigger ones are between 1.2-1.8 mm. It is worth noting that all these particles are like flakes, which means one dimension is significantly smaller than the other two dimensions.

When we used the same method to pelletize thermoplastic B, the particles we got were different from the thermoset particles as shown in Figure 4b. The first thing we noticed was that most

b

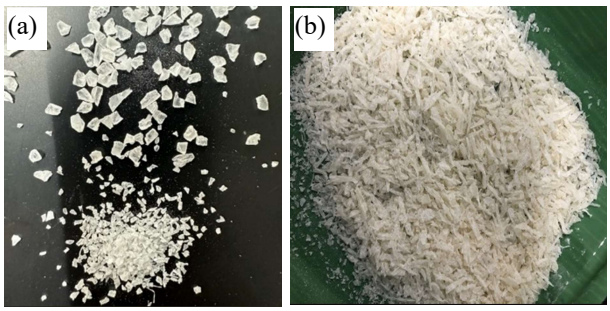

Figure 4 a) thermoset particles, separated; b) thermoplastic particles, un-separated.

fibers are from 3 mm to 12 mm. Secondly, there's much less small particles and no powder was created in the process. The lower T_g of thermoplastic B could be the reason for this. These flaky or fibrous particles are very good model particles to show the shape memory effect in lost circulation prevention as we will discuss later.

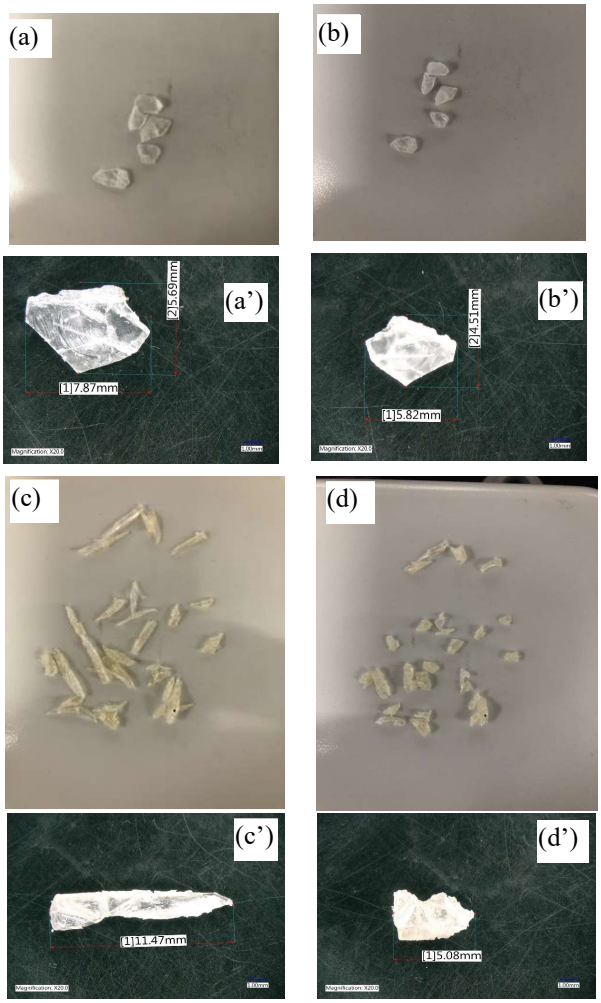

Figure 5 a & a') thermoset particles before recovery; b & b') thermoset particles after recovery; c & c') thermoplastic particles before recovery; d & d') thermoplastic particles after recovery.

Particle recovery

When we put pelletized thermoset A particles on a 140 °C hot plate, as shown in Figure 5a and 5b, these flaky particles recovered to granular like particles. The same trend happened to thermoplastic B particles as shown in Figure 5c and 5d. The short fibers became granular particles. When we measured dimension changes of these particles with a microscope, we found that the shape changes are significant even though there's no volume change in the process.

Static test

Before studying the application of shape memory functionality in leak-plugging, we must first investigate whether our material can act as a sealant without shape memory functionality, or in other words, we need to study what kind of sealing effect our material can achieve without programming.

The basic concept of all leak-plugging test methods is to create an artificial opening with a certain aperture size and then pump drilling fluid mixed with plugging particles (LCM) to the opening. The effectiveness of LCM in sealing potential cracks, holes, or super-cracks is then detected. A commonly used leak plugging test apparatus in laboratories is the PTT apparatus connected to a liquid loss receiver, as shown in Figure 1.

As discussed in the introduction part, to achieve a good sealing result, the choice of size distribution of LCM is very important. Different researchers have published different size distribution based on their geometrical shapes of particles. We have adopted a bimodal distribution of lost circulation material suggested by Razavi et al. A bimodal distribution refers to a particle size distribution primarily concentrated in two parts. One part consists of larger particles used to bridge the gaps, while the other part consists of finer particles to fill the gaps between the larger ones. A bimodal distribution of LCM can achieve reasonable crack closure, with an effectiveness depending on the filling efficiency of specific-sized particles. From literature reports, we know that most large LCM particles should be close to the average crack size. Fine LCM particles should then be synergized to the larger LCM particles. The volume ratio of fine LCM to large LCM should be approximately 1:3 to achieve optimal particle filling.

After completing the initial screening of particle sizes, we experimented by adding a total of 15 g of untreated thermosetting A particles into 350 mL 10.5 ppg water-based mud. Two-thirds of the particles were between 1.2 mm and 1.8 mm in size, while one-third were smaller than 0.6 mm in powder form. The size of the stainless-steel slot is 2-1 mm (tapered). When manually pressurizing with a hand pump, the resistance gradually increased, and the pressure indicated by the pressure gauge reached 15 MPa at room temperature. After maintaining this pressure for 30 minutes, we did not observe any leakage in the liquid receiver, indicating an excellent sealing effect of our polymer particles in the tapered slot. This might be attributed to the slight deformation of the polymer particles under high pressure, especially the finer ones, enhancing the sealing effect.

Considering the thermal expansion of the water-based mud, we maintained the pressure inside the pressure vessel at around 7 MPa once sealed at room temperature then started increasing temperature to find the highest temperature the material can seal the crack. The temperature was increased to 150 °C (302 F) with the pressure reached over 10 MPa in the sealed pressure vessel thus proving the excellent sealing capabilities of the polymer. With continued heating to 180 °C (356 F) and the pressure exceeded 13 MPa, the seal pressure was then quickly dropped to zero. This implies that the maximum operating temperature of thermoset A is around 180 °C. We assume then that when the temperature far exceeds the T_g of thermoset A, the particles gradually soften, the material modulus decreases, leading to the collapse of the originally sealed filling system.

Next, we conducted similar experiments using thermoplastic B particles. Since there were fewer fine particles generated during pelletizing for thermoplastic B, we used the fine particles from thermoset A. The experimental observations were very similar to thermoset A, showing excellent sealing when the particles sealed the gap at room temperature. However, the maximum operating temperature of thermoplastic B is 140 °C (284 F).

The above tests essentially confirmed the performance of these two materials without any shape memory programming. Next, we conducted two different experiments using programmed particles to observe the effect of shape memory functionality in leak-plugging. One method involved directly placing programmed particles into the mud for testing, allowing the particles to recover their shape inside the pressure vessel. The second method involved heating the programmed particles in an oven to induce deformation recovery before mixing them into the mud for testing.

For both methods, we kept the same particle size distribution and same stainless-steel tapered slot as previous tests. When we used programmed thermoset A particles, a tight seal was successfully initiated at room temperature. However, the pressure suddenly dropped to zero when the temperature was increased to 120 °C, which is much lower than 180 °C. Similarly, when using programmed thermoplastic B particles, sealing failed around 90 °C which is also much lower than 140 °C. Attempts to add and push through more products to achieve secondary sealing were unsuccessful for both types of particles.

In the second method, we used larger size programmed particles and a larger tapered 3-2 mm slot at the beginning. To seal 3-2 mm cracks, we selected a particle size combination consisting of 2/3 large particles (50% between 1.2 mm and 1.8 mm, and 50% between 2 mm and 2.8 mm) and 1/3 particles smaller than 0.6 mm (best described as a powder). We obtained results like those at 120 °C with 10 MPa sealing pressure in previous experiments. After completing the experiment, we continued raising the temperature to 130 °C to ensure complete shape recovery of the particles within the pressure vessel. After cooling, we replaced the 3-2 slot with 2-1 mm and began reheating and pressurizing. This time, we achieved successful resealing at 180 °C and 10 MPa.

These results indicate that for particles of same volume/size,

higher aspect ratio particles like fiber and flakes can be used to seal larger cracks or fractures. Once these higher aspect ratio particles recover and become lower aspect ratio granular, they can seal smaller cracks or fractures. This clearly demonstrates the different performance of SMP particles compared to conventional particles in lost circulation prevention applications.

Dynamic test

From the above static experiments, we can see that the deformation recovery of SMP particles makes them different from conventional LCM particles. Particles with a HAR can seal larger cracks than particles with a LAR if they are the same volume/size. If we design a scheme to allow particles with a HAR to enter relatively small cracks, these particles can continue to seal the slot after deformation. Also, if we were to present the samples with a longer wedge-shaped crack to illustrate that the particles with a HAR initially seal the larger portion of the crack. As the temperature increases to the shape recovery temperature, sealing breaks, and the particles flow to narrower sections of the crack for secondary sealing. We successfully redesigned our testing apparatus and testing slots for these two scenarios.

The new slot structure is shown in Figure 6. A funnel-shaped guiding area was added to the end of the conventional slot. This design is to facilitate the HAR particles orientating and flowing smoothly into the slot.

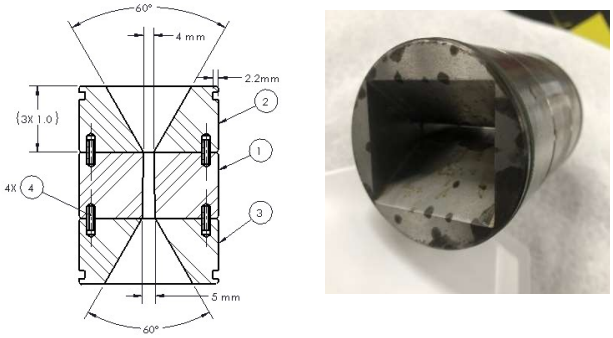

Figure 6 Slot design with a guiding piece

Programmed thermoplastic B particles with a length of about 10 mm and 1-2 mm in the other two dimensions were used in the tests. Without a guiding piece, these particles would jam at the entrance of the slot, forming a "seal gate." However, with the guiding piece, these particles could smoothly enter the fissure and form a seal. We first established a seal with the particles at room temperature, then slowly increased the temperature. When the temperature reached around 70°C, the sealing pressure suddenly dropped. While we kept increasing the temperature, we continued to pump mud through, and the pressure began to build up again. But the pressure quickly dropped again. As we kept pumping mud through, the pressure repeated several times in between building up and dropping. When the temperature reached 95 °C, no matter how much or how fast we pumped the mud, the pressure did not build up again. The entire process of pressure variation with temperature is shown in Figure 7. This continuous recovery and resealing behavior of the particles in test fixture is what we refer to as the adaptive behavior of SMPs as applied to a lost circulation prevention test.

To further demonstrate the self-adaptive performance of SMPs, we designed a long test fixture as shown in Figure 8a. This test fixture is 7.25 inches long with one end having an opening of 4 mm, while the other end having an opening of 1 mm. This kind of structure has been used by Magzouba et. al. 2021; Wang et. al., 2016 and Ravi et. al., 2006. To assemble such a long test fixture, we also made changes to our experimental set-up. As shown in Figure 8b, we connected two PPTs with a tube. One PPT was used as mud reservoir and the other was used to load the test fixture.

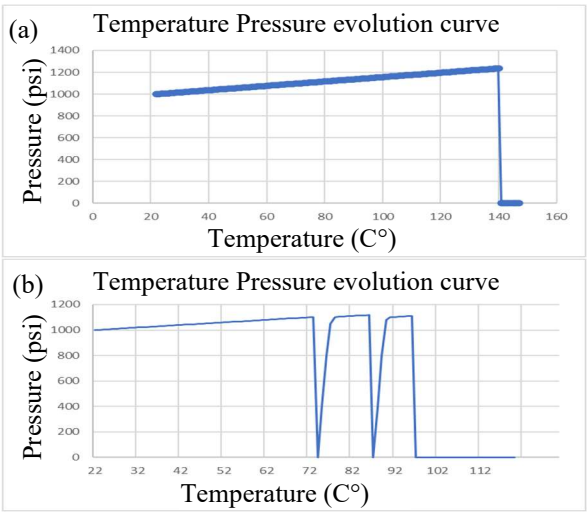

Figure 7 a) Temperature pressure evolution for thermoplastic B particles in a usual slot; b) Temperature pressure evolution for thermoplastic B particles in a test fixture with guiding piece.

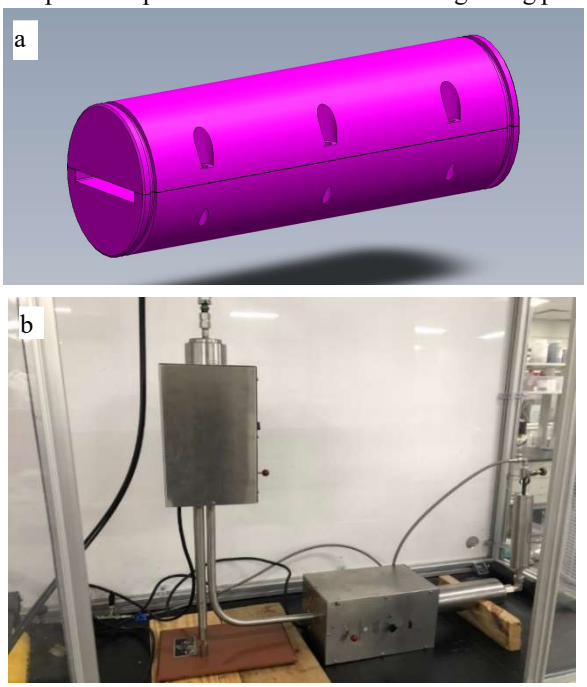

Figure 8 a) Tapered test fixture; b) modified PPT testers.

We first conducted a sealing test using programmed thermoset A particles at room temperature. After establishing pressure, we stopped the test and observed that the particles did not flow to the smallest end of the fixture, but instead, they stayed about an inch away from the end. As shown in Figure 9a, the particles were densely distributed about an inch away from the end, and this dense area was not long, indicating that the opening was quickly sealed. Once sealed, there was no more liquid flow, so there were no more particles gathering in this area.

Then we repeated the same experiment with the same size distributed particles and gradually increased the temperature to 130 °C. After the final sealing pressure was established, we stopped the test and opened the test fixture. We observed that all the dense particle regions had moved to the end of the fixture, and the dense area was longer than before as shown in Figure 9b. During the continuous deformation of the particles, the sealing continuously transitioned between dense and loose states, so it took a relatively longer time to establish the final sealing, resulting in more particles flowing into the dense area.

Figure 9 a) sealing effect before shape recovery; b) sealing effect after shape recovery.

From the results of these experiments, we can see that particles with HAR can continuously flow deeper into the cracks due to their adaptability during the process of shape recovering. This adaptive behavior of the SMP LCMs provides a new mechanism for sealing fractures with size uncertainties.

Conclusion

We have developed two types of SMPs, namely thermoset A and thermoplastic B, both of which have a good recovery rate. The T_g of thermoset A ranges from 90 °C to 120 °C, making it capable of withstanding temperatures up to 180 °C. Due to its low elongation at break of only about 20%, we used compression method for programming, achieving a recovery rate of 85%. The T_g of thermoplastic B ranges from 70 °C to 90 °C, making it capable of withstanding lower temperatures up to 140°C. With an elongation at break of around 400%, we used extension method for programming, achieving a recovery rate over 90%. Both materials were pelletized with a cutting mill followed by sieving for classification.

In static lost circulation tests, thermoset A can withstand a pressure of 10 MPa at 180 °C, while thermoplastic B can withstand a pressure of 10 MPa at 140 °C. New test fixtures were designed to demonstrate the self-adaptive behavior of SMPs in the flow channel. Programmed particles with HARs can function as regular particles when the temperature is below their recovery temperature. When temperature reaches or exceeds their transition temperature, the particles can recover and flow to the smaller opening for secondary and tertiary sealing. When combined with other particular LCMs, this adaptive feature of SMP particles would reduce the uncertainties of particle size distribution predictions by forming a secondary seal. We are currently investigating the sealing performance of SMPs combining with various granular, flaky and fibrous LCMs. The results will be published separately.

Acknowledgments

The authors acknowledge the permission of CNPC USA to publish this paper. Special thanks to Steve Vaughan for helping in setting up experiments.

Nomenclature

D(50)	Particle diameter of 50% cumulative size distribution
HAR	High Aspect Ratio
LAR	Low Aspect Ratio
LCM	Lost Circulation Material
PPT	Permeability Plug Tester
PSD	Particle Size Distribution
SMP	Shape Memory Polymer
SME	Shape Memory Effect
T_g	Glass Transition Temperature
T_{trans}	Transition Temperature

References

1. Al-Arfaj, M, Amanullah, Md., and Al-Ouhali, R, "Loss Circulation Materials Testing Methods: Literature Review" SPE-193678-MS, 12, 2018.
2. Alsaba, M, Nygaard R, Hareland, G, "Review of Lost Circulation Materials and Treatments with an Updated Classification", AADE-14-FTCE-25
3. Arun DI, Santhosh Kumar KS, Satheesh Kumar B, Chakravarthy P, Dona M, Santhosh B. High glass-transition polyurethane-caron black electro-active shape memory nanocomposite for aerospace systems. *Mater Sci Technol.* 2019; 35:596-605.
4. Dahi Taleghani A., Li, G., 2019a. Cement Materials Including Shape Memory Polymer and Methods of Making Cement Materials. U.S. Patent Application No. 16/095,058.
5. Dahi Taleghani, A., Li, G., 2018. Methods of Treating Oil and Gas Well Fractures. U.S. Patent Application No. 15/668,957.

6. Dahi Taleghani, A., Li, G., 2019b. Methods for Temporary Fracture Isolation. U.S. Patent Application No. 16/040,879.
7. Dahi Taleghani, A., Li, G., Moayeri, M., 2017. Smart expandable cement additive to achieve better wellbore integrity. J. Energy Resour. Technol. 139 (6), 062903.
8. Dahi Taleghani, A., Shojaei, A., Li, G., 2020. Shape Memory Polymer Proppants, Methods of Making Shape Memory Polymer Proppants for Application in Hydraulic Fracturing Treatments. U.S. Patent No. 10,538,694.
9. Dao TD, Ha NS, Goo NS, Yu WR. Design, fabrication, and blending test of shape meory polymer composite hinges for space deployable structures. *J Intell Mater Syst Struct*. 2018; 29:1560-1574.
10. He Q, Wang Z, Song Z, Cai S. Bioinspired design of vascular artificial muscle. *Adv Mater Technol*. 2019; 4:1800244
11. Howard, G. C., and Scott, P. P. 1951. "An Analysis and the Control of Lost Circulation". SPE-951171-G. Journal of Petroleum Technology. Vol. 3, No. 6, 171-182.
12. Lee Lu and Taleghani Arash Dahi, "The Effect Particle Size Distribution of Granular LCM on Fracture Sealing Capability". SPE-201668-MS, 2020.
13. Liu Y, Du H, Liu L, et al. Shape memory polymers and their composites in aerospace applications: a review. *Smart Mater Struct*. 2014; 23:023001.
14. Loeppke, G., Glowka, D., Wright, E.; Design and Evaluation of Lost-Circulation Materials for Severe Environments, Journal of Petroleum Technology, March 1990
15. Magzoub Musaab, Salehi,Saeed, Li Gouqiang, Fan Jizhou, Teodoriu Catalin Geothermics 89(2021) 101943.
16. Nayberg, T. M. and Petty, B. R. "Laboratory Study of Lost Circulation Materials for use in Both Oil-base and Water-base Drilling Muds". IADC/SPE 14723, IADC/SPE Drilling Conference, Dallas, USA, 10-12 February 1986.
17. Prathumrat,Peerawat Nikzad Mostafa, Hajizadeh Elnaz, Arablouei Reza, Sbarski Igor "Shape memory elastomers: A review of synthesis, design, advanced manufacturing, and emerging applications" Polym Adv Technol. 2022;33:1782–1808
18. Ravi, K., Savery, M., Reddy, B., Whitfill, D.; Cementing Technology for Low Fracture Gradient and Controlling Loss Circulation, paper SPE 102074 prepared for presentation at the SPE/IADC Indian Drilling Technology Conference and Exhibition held in Mumbai, India, 2006
19. Razavi Omid, Vajargah Ali Karimi, Van Oort Eric, Aldin Munir, "Optimum particlesize distribution design for lost circulation control and wellbore strengthening". Sudarshan Govindarajan Journal of Natural Gas Science and Engineering, Volume 35, Part A, September 2016, Pages 836-850
20. Santos, L., Dahi Taleghani, A., Li, G., 2017. Expandable diverting agents to improve efficiency of refracturing treatments, SPE/AAPG/SEG Unconventional Resources Technology Conference. no. 2016.
21. Santos, L., Dahi Taleghani, A., Li, G., 2018a. Expandable proppants to moderate production drop in hydraulically fractured wells. J. Nat. Gas Sci. Eng. 55, 182–190.
22. Santos, L., Dahi Taleghani, A., Li, G., 2018b. Smart expandable polymer cement additive to improve zonal isolation. In: Proceedings of the SPE Eastern Regional Meeting, p. 9.
23. Santos, L., Dahi Taleghani, A., Li, G., 2020a. Smart expandable fiber additive to prevent formation of microannuli. SPE Drill. Compl. 1–13.
24. Santos, L., Dahi Taleghani, A., Li, G., 2020b. Nanosilica-treated shape memory polymer fibers to strengthen wellbore cement. J. Pet. Sci. Eng. 196. 107646.
25. Schlumberger. 2014. Oil Field Glossary, http://www.glossary.oilfield.slb.com (Accessed 24 January 2014)
26. Shojaei Amir, Jamison Dale E., "Use of shape memory materials in wellbore servicing fluids". U. S. Patent No. 10570330B2, 2020.
27. Tran. V.T., Civan. F. and Robb. I.: "Correlating flowing time and condition for perforation plugging by suspended particles." SPE 120473, SPE Production and Operations Symposium, Oklahoma, U.S.A, 4-8 April 2009.
28. Van Oort, E., Friedheim, J., Pierce, T., and Lee, J. "Avoiding Losses in Depleted and Weak Zones by Constantly Strengthening Wellbores". SPE 125093, SPE Annual Technical Conference and Exhibition, New Orleans, Louisiana, USA, 4-7 October 2009.
29. Wang Gui, Cao Cheng, Pu Xiaolin and Zhao Zhengguo, "Experimental investigation on plugging behavior of granular lost circulation materials in fractured thief zone", Particulate Science and Technology 2016, VOL. 34, NO. 4, 392–396.
30. Wang Xiuli and Osunjave Gbenga, "Advancement in Openhole Sand Control Applications Using Shape Memory Polymer", SPE ATCE 2016.
31. Whitfill, D.L. and Hemphill, T., "All Lost-Circulation Materials and Systems Are Not Created Equal" Paper SPE 84319 prepared to be presented at the 2003 SPE Annual Technical Conference and Exhibition held in Denver, Colorado, October 5-8.
32. Withfill, D. L. "Lost Circulation Material Selection, Particle Size Distribution and Fracture Modeling with Fracture Simulation Software". IADC/SPE 115039, IADC/SPE Asia Pacific Drilling Technology Conference and Exhibition, Jakarta, Indonesia, 25-27 August 2008.
33. Worch JC, Weems AC, Yu J, et al. Elastomeric polyamide biomaterials with stereochemically tuneable mechanical properties and shape memory. *Nat Commun*. 2020; 11:1-11.
34. Xiao M, Zhang N, Zhuang J, et al. Degradable poly (ether-ester-urethane) s based on well-defined aliphatic diurethane diisocyanate with excellent shape recovery properties at body temperature for biomedical application. *Polymer*. 2019;11:1002.